For the purposes of designing the input and output matching networks for RF power amplifiers, one-port impedance models can be more effective than two-port device models.

One-Port Impedance Models Prove Useful for Broadband RF Power Amplifier Design

By
Tom Apel
Acrian, Inc.

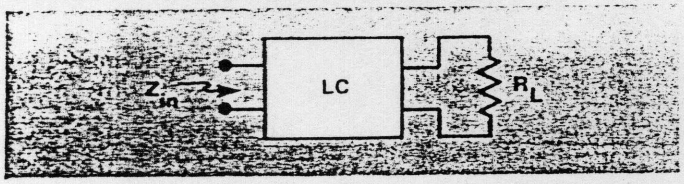

1. In order to obtain a form compatible with a subsequent synthesis step, all one-port models are considered to be two-port LC networks which are resistively terminated.

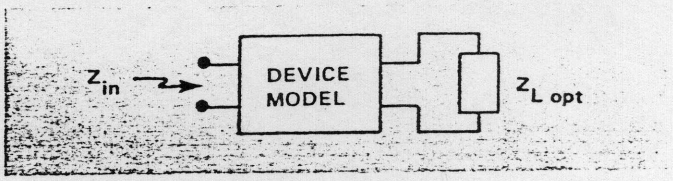

2. In this two-port representation, the output provides an optimum load and Z_{in} results at port 1. The input interface is conjugate matched.

When one considers RF power device modeling methods, a broad range of techniques come to mind along with the question of which is best. The purpose of all models is to represent the behavior of a physical system. The more complete the representation, the more complicated the model usually becomes. The form of a model (i.e., the information which is conveyed) is governed by the needs of the application. In other words, there is no one device model which optimally addresses the needs for all applications.

For example, in order to optimize the design of a new device, the designer requires a two-port representation in which individual electrical elements within the model each have physical significance.[1,2,3,4,5] The non-linear behavior of the two-port representation can be included either quasi-statically,[6,7,8,9] or by a time-domain representation.[10,11,12] These representations are also useful to the circuit designer for simulating harmonic and intermodulation distortion (IMD) behavior. However, in order to design the input and output matching networks, the two-port device model is not the best choice.

The purpose here is to present a method with which one-port impedance models can be obtained. Since the input and output matching networks must provide desired interface impedance behavior, the effective input and output impedance of the device can be represented as the complex conjugate of those optimum terminations. Due to the non-linear behavior of the active device, the optimum interface impedances are best determined by application of load-pull techniques.[13]

One- and Two-Port Transistor Models

Usually, RF power amplifier device characterization does not include full two-port characterization, due to the non-linear behavior of the device. However, large signal S-parameters can be obtained by the two-signal method.[13] If the system reference impedance, R_o, is near the operating impedance level, then the two-port representation can be meaningful and useful.

When the optimum load impedance is denoted as Z_L, the optimum load reflection coefficient is given by Equation 1. Equation 2 gives the corresponding device input reflection coefficient.

$$\rho_L = \frac{Z_L - R_o}{Z_L + R_o} \qquad (1)$$

$$\rho_{in} = S_{11}' = S_{11} + \frac{S_{12}\, S_{21}\, \rho_2}{1 - S_{22}\, \rho_2} \qquad (2)$$

Tom Apel is a staff scientist with Acrian, Inc., 10060 Bubb Road, Cupertino, CA 95014; (408) 996-8522.

When rewritten in impedance form, Equation 2 leads to Equation 3.

$$Z_{in} = R_o \frac{1 + S_{11}'}{1 - S_{11}'} \qquad (3)$$

It should be kept in mind that Z_{in} is usually obtained by direct measurement[13] or indirect (source-pull) means, rather than with large-signal S-parameters. The one-port representation is predicated on the presence of conjugate match at both device ports. This allows both matching networks to be synthesized from the respective one-port load models. A more proper label for the output model might be "effective output model," since it is only an artificial tool with which the output matching network is obtained.

Previous efforts to obtain one-port impedance models have included the use of negative element models and numerical optimization.[14] This is equivalent to obtaining a one-port model by optimization of the positive element model which is terminated with complex conjugate device data. In contrast, the approach taken here does not rely upon numerical optimization to obtain the model, since closed-form equations exist.

In order to provide a form which is compatible with the subsequent synthesis step, all one-port models are considered to be two-port LC networks which are resistively terminated. This is illustrated in Figure 1. It should be noted that no restrictions are placed on the LC structure of the model, such that individual circuit elements have physical significance. Since our ultimate goal is to design an impedance matching network, the two most important constraints placed on the load model are those of a synthesis compatible form and accurate representation of measured data. To clarify this, consider Figure 2. The output network provides an optimum load and Z_{in} results at port 1. The input interface is conjugate matched. However, the output interface is usually not conjugate matched for RF power amplifiers.

As with small-signal amplifiers, intrinsic (e.g., C_{ob}) and extrinsic (e.g., bond wires) reactive effects must be matched out. The difference between RF power amplifier output loading and that of conjugate matched small-signal amplifiers is in the real part of the load impedance, at the intrinsic terminals. With RF power amplifiers, this real load is dependent on the operating voltage and available current. Hence, while the behavior of the output port impedance in Figure 3 does not represent the device output exactly, it does accurately represent the optimum interface impedance. For this reason, one might prefer to call the one-port representation of port two an effective impedance model.

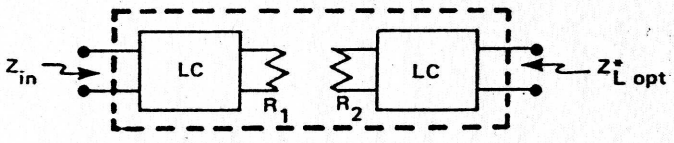

EFFECTIVE Z DEVICE MODEL

3. In RF power amplifiers, the real load is dependent on the operating voltage and the available current, so the behavior of the output port impedance shown here does not represent the device output exactly; it does, however, accurately represent the optimum interface impedance.

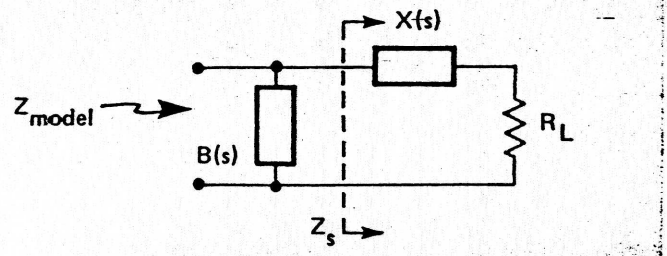

a.) SERIES BEHAVIOR WITH SHUNT PERTUPBATION

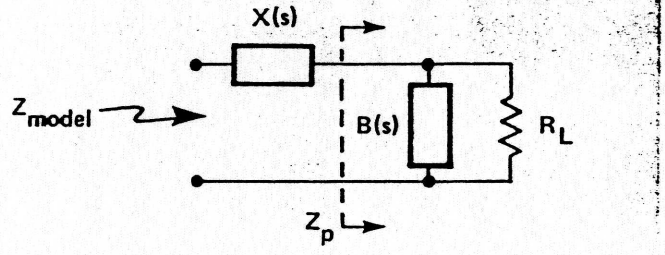

b.) SHUNT BEHAVIOR WITH SERIES PERTURBATION

4. In the two one-port topologies being considered, each reactance or susceptance block is allowed up to second-order behavior. This means that fourth-order models can be realized.

One Port Realization

In order that the form of the one-port model is compatible with the subsequent matching network synthesis step, we will require all losses to be lumped into a single resistor which terminates an LC two-port. Figure 4 illustrates the two topologies being considered here. Each reactance or susceptance block will be allowed up to second-order behavior. Hence, fourth-order models can thereby be realized. Occasionally, the need arises for higher-order load models, and the approach which is presented here can be easily extended to cover those cases. For example, "T" or "π" sixth-order models can be obtained with the addition of one series or shunt block to the forms represented in Figure 4.

Since the simplified models of Figure 5 each contain three unknowns, a minimum of three datum points are required to form a solution. In order to be representable with the one-port forms of Figure 5, the datum points must fall along a constant resistance or constant conductance contour with monotonic reactance or susceptance

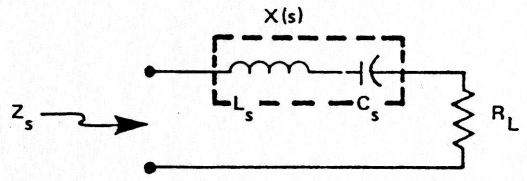

a.) SERIES BEHAVIOR (NO PERTURBATION)

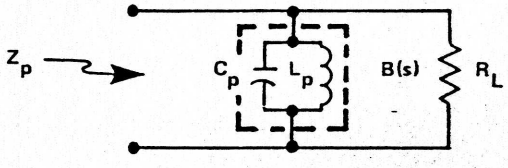

b.) SHUNT BEHAVIOR (NO PERTURBATION)

5. Owing to the fact that these simplified models each contain three unknowns, a minimum of three datum points are required to form a solution.

behavior, respectively. Data which does not fall into either of these two categories cannot be adequately represented with the simplified (Fig. 5) forms. The more complex forms (Fig. 4) will be considered later. The termination resistance, R_L, can be set by calculating the average resistance (series form) or average conductance (shunt form). The LC solution can be determined from the total reactance (series) or susceptance which is desired at the band-edge frequencies. This is done as follows:

$$L_s = \frac{f_2 X_2 - f_1 X_1}{2\pi (f_2^2 - f_1^2)} \quad (4)$$

$$C_s = \frac{f_2^2 - f_1^2}{2\pi (f_1^2 f_2 X_2 - f_1 f_2^2 X_1)} \quad (5)$$

$$L_p = \frac{f_2^2 - f_1^2}{2\pi (f_1^2 f_2 B_2 - f_1 f_2^2 B_1)} \quad (6)$$

and

$$C_p = \frac{f_2 B_2 - f_1 B_1}{2\pi (f_2^2 - f_1^2)} \quad (7)$$

where f_1 = Lower band edge
f_2 = Upper band edge
$X_1 = X(f_1)$
$X_2 = X(f_2)$
$B_1 = B(f_1)$
and $B_2 = B(f_2)$

The simplest forms are, of course, the single inductor or capacitor, either in series or parallel with R_L. Unfortunately, these forms do not adequately represent the broadband impedance behavior of many RF power devices. If they did, there would be no need for this article. As a preliminary step, consider the forms of Figure 4 in which the perturbing block has been removed. These

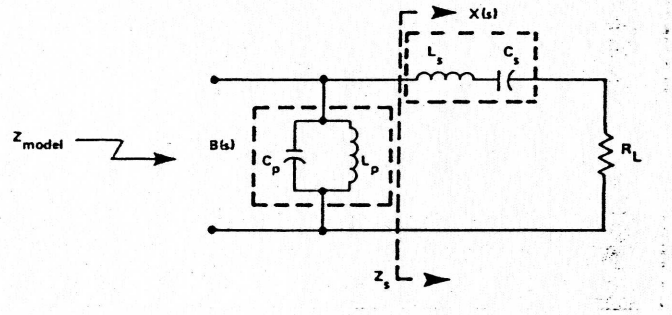

6. The fourth-order bandpass realization is shown for the one-port series model with shunt perturbation.

forms are shown in Figure 5, with bandpass LC-effects allowed (N = 2).

As long as $f_2 X_2 > f_1 X_1$ and $f_1 X_2 > f_2 X_1$, L_s and C_s will remain positive. Similarly, for $f_2 B_2 > f_1 B_1$ both L_p and C_p are positive. However, at this point we will not require that the LC solutions be strictly positive, since a negative element is always removable from the simple one-port forms by externally applying a larger positive element of the same type. When the fourth-order forms

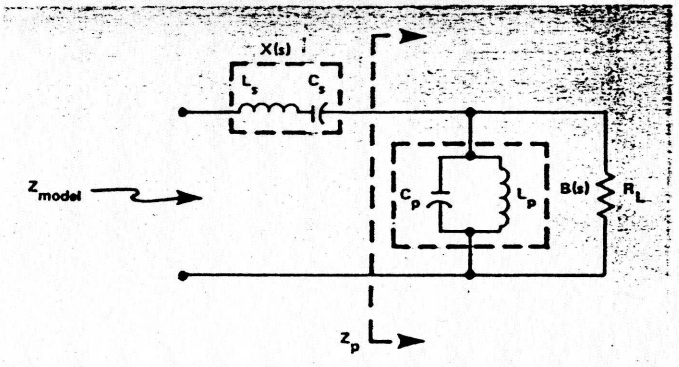

7. The fourth-order bandpass realization can be seen for the one-port shunt model with series perturbation.

of Figure 4 are considered, only perturbing elements which are available at the accessible terminals are allowed to be negative valued. It is a consequence of the $dX(\omega)/d\omega > 0$ rule for realizable LC network driving-point impedance behavior that positive LC values are always associated with clockwise movement around a region on the Smith chart, with increasing frequency. We next make use of this fact in order to choose the correct topology from Figure 4.

The fourth-order bandpass realizations of Figure 4(a) and Figure 4(b) are illustrated in Figures 6 and 7, respectively. The subnetworks, with driving-point impedances Z_s and Z_p are obtained with Equations 4, 5, 6, and 7, and a procedure identical to that which was applied to the networks of Figure 5. The additional task, which is required for solutions to the networks of Figures 6 and

7, is to first decompose the desired model's behavior into simplified form (Fig. 5) and necessary perturbation. The perturbing effects often tend to be the greatest at the band edges. However, this will depend ultimately on the selection of R_L. Before any guidelines for this decomposition are stated, consider a typical case.

Figure 8 illustrates a shunt-perturbed, series-resonant case. This particular case happens to be approximately midband resonant, which is desirable for impedance matching. Figure 8 provides a view of both the modeled behavior and subnetwork behavior, Z_s (dashed locus). By inspection, the Smith chart yields the shunt perturbations at the band edges, B_1 and B_2. The end points are therefore fixed. The selection of R_L controls the amount of curvature in the locus. Usually R_L is set to the lowest value which is encountered in the real part of the data to be modeled with this topology. In the example of Figure 8, this occurs near midband.

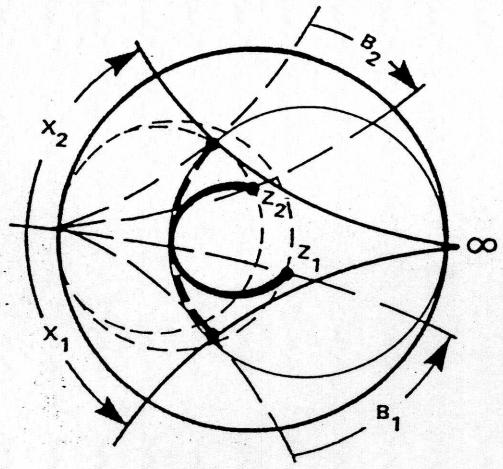

8. This shunt-perturbed, series-resonant case is approximately midband resonant, which is desirable for impedance matching.

Conversely, when a series perturbed-shunt model is used, the selection of R_L is determined by the largest value in the real part of the data to be modeled. Unfortunately, these selection guidelines not only provide a good data fit, but they also tend to maximize the Q of the principal part of the model. This, of course, is in the direction contrary to enhancement of broadbandability. (This is nature's way of reminding us not to expect something for nothing!)

Figure 9 provides an example of the series perturbed-shunt resonant case. As in Figure 8, the modeled locus is represented with a solid line. The subnetwork behavior, Z_p, is represented with a dashed line. Once again, the perturbations at the band edges, X_1 and X_2, can be determined by inspection.

RF power amplifier device characterization usually does not include full two-port characterization.

Most load model requirements for broadband amplifier design can be easily provided with the two fourth-order cases. Single-loop resonances can be addressed with this approach. Loci which are not midband resonant are realized in the same manner as the midband resonant cases of Figures 8 and 9. However, the component values which are realized usually allow a simplification of the model. That is, when series or shunt-resonant branches are very far from resonance in the band of interest, one element usually dominates in the behavior of that branch. The order of the model can, thereby, be reduced. The closed-form expressions for fourth-order models are as follows:

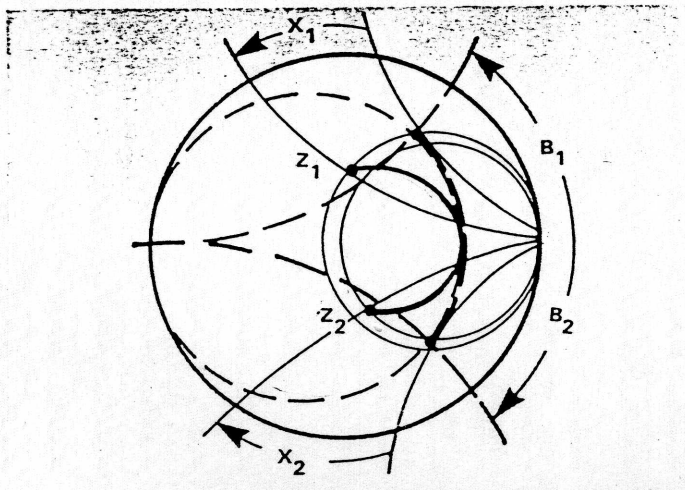

9. In this series perturbed-shunt resonant case, the model locus is represented with a solid line and the subnetwork behavior (Z_p) with a dashed line.

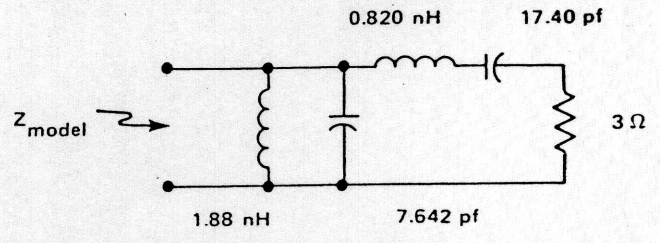

10. This series resonant model with a shunt perturbation is based on the data in the Table.

Shunt With Series Perturbation

$$B_1 = \frac{A\sqrt{\frac{R_L}{R_A} - 1}}{R_L} \tag{8}$$

$$X_1 = X_A + AR_A\sqrt{\frac{R_L}{R_A} - 1} \tag{9}$$

$$B_2 = \frac{B\sqrt{\frac{R_L}{R_B} - 1}}{R_L} \tag{10}$$

$$X_2 = X_B + BR_B\sqrt{\frac{R_L}{R_B} - 1} \tag{11}$$

where

$$Z(f_1) = R_A + jX_A$$
$$Z(f_2) = R_B + jX_B$$

$$A = \begin{cases} +1, \text{ if Imag}\{Z_p(f_1)\} \leq 0 \\ -1, \text{ if Imag}\{Z_p(f_1)\} > 0 \end{cases}$$

and

$$B = \begin{cases} +1, \text{ if Imag}\{Z_p(f_2)\} \leq 0 \\ -1, \text{ if Imag}\{Z_p(f_2)\} > 0 \end{cases}$$

Series With Shunt Perturbation

$$X_1 = AR_L\sqrt{\frac{R_A(1+Q_1^2)}{R_L} - 1} \tag{12}$$

$$B_1 = \frac{A\sqrt{\frac{R_A(1+Q_1^2)}{R_L} - 1}}{R_A(1+Q_1^2)} - \frac{Q_1^2}{X_A(1+Q_1^2)} \tag{13}$$

$$X_2 = BR_L\sqrt{\frac{R_B(1+Q_2^2)}{R_L} - 1} \tag{14}$$

$$B_2 = \frac{B\sqrt{\frac{R_B(1+Q_2^2)}{R_L} - 1}}{R_B(1+Q_2^2)} - \frac{Q_2^2}{X_B(1+Q_2^2)} \tag{15}$$

where

$$Z(f_1) = R_A + jX_A$$
$$Z(f_2) = R_B + jX_B$$

$$Q_1 = \left|\frac{X_A}{R_A}\right|$$

$$Q_2 = \left|\frac{X_B}{R_B}\right|$$

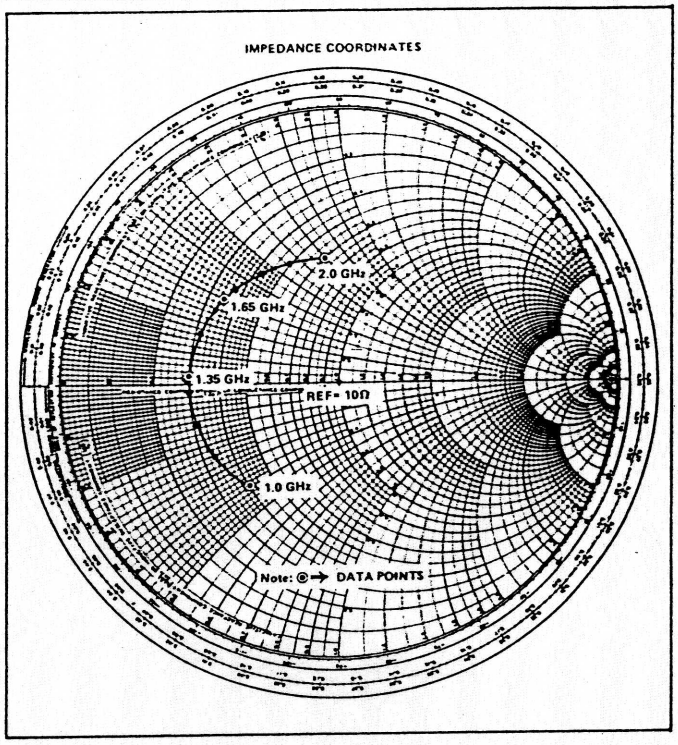

11. The corresponding impedance for the model in Figure 10 is seen to be quite good.

$$A = \begin{cases} -1, \text{ if Imag}\{Z_s(f_1)\} \leq 0 \\ +1, \text{ if Imag}\{Z_s(f_1)\} > 0 \end{cases}$$

and

$$B = \begin{cases} -1, \text{ if Imag}\{Z_s(f_2)\} \leq 0 \\ +1, \text{ if Imag}\{Z_s(f_2)\} > 0 \end{cases}$$

An Example

As a numerical example, consider the data which is listed in the Table. We note that the data is similar to the case illustrated in Figure 8. Hence, we will use a series resonant model, with a shunt perturbation. Since the minimum real part of the data in the Table is 3.0 Ohms, we will set $R_L = 3$ Ohms. By Equations 12, 13, 14, and 15 we obtain the following:

$X_1 = -3.873$
$B_1 = -0.0364$
$X_2 = +5.788$
$B_1 = +0.0538.$

The element values within the model are then obtained from Equations 4, 5, 6, and 7. Figure 10 illustrates the complete model. The corresponding impedance performance shown in Figure 11 is good.

Table
Numerical Example Data

Freq. (GHz)	R_{Load}	X_{Load}
1.00	4.0	-4.0
1.35	3.0	0.0
1.65	3.5	3.0
2.00	6.0	7.0

A method has been developed for obtaining one-port impedance models with closed-form equations. These equations allow fourth-order solutions. The techniques presented here can be extended to accommodate higher order models, where required. One-port load models are a necessary prerequisite for the broadband matching synthesis techniques which will be considered in a subsequent article. ■

References

1. Cooke, "Microwave Transistors: Theory and Design," *Proceedings IEEE* (Vol. 59), Aug. 1971, pp. 1163-1181.
2. Chen and Snapp, "Bipolar Microwave Linear Power Transistor Design," *IEEE Trans. MTT-27*, May 1979, pp. 423-430.
3. East and Haddad, "GaAs FET Device Modeling and Performance," *AFWAL Rep. TR-81-1191*, Nov. 1981.
4. Peck and Peterson, "A Measurement Method for Accurate Characterization and Modeling of MESFET Chips," *IEEE MTT-S International Microwave Symposium 1981*, pp. 310-312.
5. Madjar and Rosenbaum, "A Large-Signal Model for the GaAs MESFET," *IEEE Trans. MTT-29*, Aug. 1981, pp. 781-788.
6. Soares, et al., "Non-Linear Equivalent Circuit for Broadband GaAs MESFET Power Amplifier Design," *IEEE MTT-S International Microwave Symposium 1982*, pp. 63-65.
7. Rauscher and Willing, "Simulation of Non-Linear Microwave FET Performance Using a Quasi-Static Model," *IEEE Trans. MTT-27*, Oct. 1979, pp. 834-840.
8. Gupta, et al., "Frequency Multiplication with High-Power Microwave Field-Effect Transistors," *IEEE MTT-S International Microwave Symposium 1979*, pp. 498-500.
9. Camargo, et al., "Sources of Non-Linearity in GaAs MESFET Frequency Multipliers," *IEEE MTT-S International Microwave Symposium 1983*, pp. 343-345.
10. Peterson, et al, "A GaAs FET Model for Large-Signal Applications," *IEEE Trans. MTT-32*, March 1984, pp. 276-281.
11. Vidkjaer, "A Describing Function Approach to Bipolar RF Power Amplifier Simulation," *IEEE Trans. CAS-28*, Aug. 1981, pp. 758-767.
12. Vidkjaer, "Instabilities in RF Power Amplifiers Caused by a Self-Oscillation in the Transistor Bias Network," *IEEE Journal SC-11*, Oct. 1976, pp. 703-712.
13. Apel, "RF Power Device Characterization Accomplished Through Direct and Indirect Techniques," *Microwave Systems News*, Sept. 1984, pp. 115-134.
14. Medley and Allen, "Broadband GaAs FET Amplifier Design Using Negative Image Device Models," *IEEE Trans. MTT-27*, Sept. 1979, pp. 784-787.
15. Manley and Rowe, "Some General Properties of Non-Linear Elements—Part I. General Energy Relations," *Proceedings IEEE*, July 1956, pp. 704-913.

Reprinted from the October 1984 issue of Microwave Systems News